

Probing the anomalous tqgamma couplings in photon-proton collisions

E. Alici*

Department of Physics, Zonguldak Bulent Ecevit University, Turkey

arXiv:2203.14682v1 [hep-ph] 28 Mar 2022

Abstract

The top quark flavor changing neutral current processes are extremely suppressed within the Standard Model. Nevertheless, they could be enhanced in a new physics model beyond the Standard Model. Investigating the top quark's flavor changing neutral current interactions at colliders would be an important test in terms of new physics. In this work, we examine the potentials of the processes $e^-p \rightarrow e^- \gamma^* p \rightarrow e^- W^+ b \gamma^* \rightarrow e^- j \bar{j} b \gamma^*$ and $e^-p \rightarrow e^- \gamma^* p \rightarrow e^- W^+ b \gamma^* \rightarrow e^- \nu_l b \gamma^*$ at the FCC-eh with $\sqrt{s} = 7.08$ and $10.0 TeV$ to study anomalous $tq\gamma$ couplings via effective Lagrangians. We obtain 95% confidence level sensitivities on the anomalous coupling parameters at the three FCC-eh energies and various integrated luminosities. We find that our limits are at least two orders of magnitude better than the current LHC experimental results.

PACS numbers: 14.60.Fg

I. INTRODUCTION

The Standard Model (SM) is an excellent theory that defines subatomic particles and their fundamental interactions together. As a result of the discovery of all the foreseen particles by the SM including Higgs boson, it has been proved to be a correct and powerful theory for particle physics[1, 2]. However, it can be considered as an effective model of an extended theory owing to some of its important deficiencies. In this context, various extended theories which are called beyond the Standard Model (BSM) such as Supersymmetry, Extra Dimensions, Little Higgs, model standard model effective lagrangian theory(SMEFT) etc. have been proposed. Top quark interactions play a key role and provide very unique exploration opportunities to extended theories due to their huge mass nearly the same amount with the electroweak scale, for the examination of these theories.[3]

A salient feature of the usual top quark sector is that the Flavor Changing Neutral Current (FCNC) transitions are exceedingly weak as a result of the Glashow-Iliopoulos-Maiani (GIM) mechanism. According to the GIM mechanism, these interactions are prohibited at tree-level and are immensely repressed at the loop-level. The whole of these transitions in the SM are much beneath the detectable level by experiment, e.g. anticipated branching ratio for decays

* edaalici@beun.edu.tr

of $t \rightarrow q\gamma$ ($q=u, c$) are about 10^{-14} . But, in the BSM theories, the GIM mechanism commonly doesn't effective as much as in the SM. Therefore FCNC effects are at a measurable level at the high energy particle colliders. Hence, investigation of these unusual decay channels of the top quark would be evidence of extended theories.[6–14] In the literature, there are various experimental and phenomenological works about FCNC couplings of the top quark to photon and u or c quark via the SMEFT.[15–53] Up to date, different collaborations have achieved constraints on the branching fractions of top quark FCNC transitions.[40–53] The strongest limits related to the anomalous FCNC $tq\gamma$ interactions have obtained by the ATLAS collaborations at the LHC. The most restrictive experimental constraints on the branching fraction, via left-handed(right handed) $tq\gamma$ couplings have been achieved as $BR(t \rightarrow u\gamma) < 2.8 \times 10^{-5}(6.1 \times 10^{-5})$ and $BR(t \rightarrow c\gamma) < 22 \times 10^{-5}(18 \times 10^{-5})$ [53]. Despite many experimental researches, there haven't been found any hint for anomalous FCNC transitions of the top quark, at the present colliders. Therefore, future particle colliders, which are planned to have new technologies and different type of collisions than present accelerators, are gaining importance in the FCNC researches.

The LHC, the available most powerful and highest resolution collider, will complete its mission in the 2030s. According to the conceptual design report (CDR) revealed by CERN in 2012 and revised in 2017, a new collider called Future Circular Collider (FCC) will be built in the post-LHC area. FCC is designed as a proton-proton collider with a 100 TeV centre-of mass energy [54–57]. Furthermore, the FCC will have different interaction possibilities. Moreover, electron-proton and photon-proton interactions will be possible thanks to a special electron linear collider (ERL) that will be built tangentially to the ring-shaped main tunnel of the FCC. That collider is called FCC-eh has three different centre-of mass energy options. In this investigation, two of them 7.08 TeV and 10.0 TeV has been taken into account. Although electron-proton and photon-proton collider type have lower centre-of mass energy than pp collider, they enable a clean background independent of the pile-up and multiple interactions that are formed as a result of strong interaction in pp processes. Hence, they are of great importance in order to examine the main structure of matter.

In this paper, the photon-proton processes, in which the electron formed a photon, are taken into consideration. The photons, which are named quasi-real photons, arise from spontaneous radiation of the ERL electron beam. The electron beam moving in the special linac loses some of its transverse momentum and emitting of photons scattered from the

direction of movement at a very small angle. These photons are consistent with Weizsacker-Williams approximation (WWA)[58–60].

II. THEORETICAL FORMALISM

FCNC transitions can be possible via the Standard Model Effective Field Theory (SMEFT) relied on effective low energy lagrangian which has the same symmetry group with the SM. With the new terms added to the SM lagrangian, effective lagrangian is defined as the following form,[63, 64]

$$\mathcal{L} = \mathcal{L}_{SM}^{(4)} + \sum_{n=1} \frac{1}{\Lambda^n} \mathcal{L}^{(n+4)} + h.c.. \quad (1)$$

here $\mathcal{L}^{(n+4)}$ contains operators of dimension $n+4$ produced by the SM fields, \mathcal{L}_{SM} is defined the SM Lagrangian and Λ is the energy scale of extended theories. In this paper, we have considered using the second order in terms of the new physics which is the dimension six operators describing FCNC couplings amongst the top quark, q and photon. The SM Lagrangian can be extended easily with the FCNC couplings in the vertex of $tq\gamma$ as follows[62],

$$\mathcal{L} = \frac{g_e}{2m_t} \sum_{q=u,c} \bar{q} \sigma_{\mu\nu} (\lambda_{qt}^R P_R + \lambda_{qt}^L P_L) t A^{\mu\nu} + h.c \quad (2)$$

In the above equation, $\sigma_{\mu\nu} = [\gamma_\mu, \gamma_\nu]/2$, g_e symbolizes the electromagnetic coupling constant. $\lambda_{qt}^{R(L)}$ are dimensionless real parameters which stand for the anomalous couplings constant $\lambda_{qt}^R = \lambda_{qt}^L = \lambda_q$. Additionally, in our paper, λ_{ut} and λ_{uc} has been considered as equal. Utilizing Eq(2), decay width of the anomalous $tq\gamma$ couplings can easily obtained as $\Gamma(t \rightarrow q\gamma) = \frac{\alpha}{2} \lambda_q^2 m_t \simeq 0.6528 \lambda_q^2$. In the SM, the primary decay channel of the top quark sector is in the mode which a W boson and a b quark are produced. The decay width of this channel is approximately 1.49 GeV. Based on these data, the branching ratio of anomalous couplings can be written as fraction of $t \rightarrow q\gamma$ ($q=u,c$) decay width to $t \rightarrow Wb$ decay width. Consequently, it can be easily get as $Br(t \rightarrow q\gamma) = 0.4573 \lambda_q^2$.

III. CROSS SECTIONS

In this paper, we have examined $e^-p \rightarrow e^- \gamma^* p \rightarrow e^- W^+ b \gamma^* \rightarrow e^- j \bar{j} b \gamma^*$ ($j = u, d, b, c, s$ and $\bar{j} = \bar{u}, \bar{d}, \bar{b}, \bar{c}, \bar{s}$) and $e^-p \rightarrow e^- \gamma^* p \rightarrow e^- W^+ b \gamma^* \rightarrow e^- l \nu_l b \gamma^*$, ($l = e, \mu$ and $\nu_l = \nu_{e, \mu}$), processes via the SMEFT. In figures and tables, $e^-p \rightarrow e^- \gamma^* p \rightarrow e^- W^+ b \gamma^* \rightarrow e^- l \nu_l b \gamma^*$ processes are mentioned as leptonic channel and $e^-p \rightarrow e^- \gamma^* p \rightarrow e^- W^+ b \gamma^* \rightarrow e^- j \bar{j} b \gamma^*$ as hadronic channel. To generate these processes, we utilized the Monte Carlo simulation program MadGraph 5 aMC@NLO [65]. We expanded The FeynRules package, in which the Standard Model lagrangian is defined, by adding Universal FeynRules Output (UFO) modul that inculuding SMEFT lagrangian terms. [66]. In this UFO modul, SM-ckm matrix have been taken diagonal. However, in the processes we are interested in, the mixing between the first and second generation quark family must be allowed. Therefore, we embedded ckm matrix elements into the program.

For analysis, we have chosen the CTEQ6L1 parton distribution function because it also has WW photon distribution function.

For the $\gamma^* \gamma^*$ processes, the EPA photon distribution function is given by [58–61],

$$f_{\gamma^*}(x) = \frac{\alpha}{\pi E_e} \left\{ \left[\frac{1-x+x^2}{x} \right] \log\left(\frac{Q_{max}^2}{Q_{min}^2}\right) - \frac{m_e^2 x}{Q_{min}^2} \left(1 - \frac{Q_{max}^2}{Q_{min}^2}\right) - \frac{1}{x} \left[1 - \frac{x}{2}\right]^2 \log\left(\frac{x^2 E_e^2 + Q_{max}^2}{x^2 E_e^2 + Q_{min}^2}\right) \right\}$$

where $x = \frac{E_{\gamma^*}}{E_e}$ and Q_{max}^2 is the maximum virtuality of the photon. During the calculation, the photon virtuality is taken as $Q_{max}^2 = 2 \text{ GeV}^2$. The minimum value of Q_{min}^2 is given as follows

$$Q_{min}^2 = \frac{m_e^2 x}{1-x} \quad (4)$$

For the processes in this study, we applied different cutoffs to make the distinction of the SM cross section with the new physics clearer. For this purpose, we first applied $p_t^{l, \nu_l, b, j, \bar{j}} > 20$ and $|\eta|^{l, b, j, \bar{j}, \gamma} < 2.5$ for the cut off named cut1. Here, p_t is the transverse momenta of the relevant particles while η is the pseudorapidity. In addition, the four different transverse momentum values of the photon, which is the final state particle, $p_t^\gamma > 20 \text{ GeV}$, $p_t^\gamma > 30 \text{ GeV}$, $p_t^\gamma > 40 \text{ GeV}$ and $p_t^\gamma > 50 \text{ GeV}$ have been applied together with cut1, and these cut-offs are named as cut2, cut3, cut4 and cut5, respectively. By applying these different cut offs, we investigated the suppressing effect of the photon's transverse momentum on the SM cross section. The relevant cuts are given in Table 1.

TABLE I. cuts.

Cut1	$p_t^{l,\nu_l,b,j,\bar{j}} > 20, \eta ^{l,b,j,\bar{j},\gamma} < 2.5$
Cut2	$\text{Cut1} + p_t^\gamma > 20$
Cut3	$\text{Cut1} + p_t^\gamma > 30$
Cut4	$\text{Cut1} + p_t^\gamma > 40$
Cut5	$\text{Cut1} + p_t^\gamma > 50$

In this regard, SM cross section values were calculated and the ratios of the obtained these values to the total cross section values calculated for the new physics parameter ($\lambda=0.01$) value were found. Thus, we determined which of the used cuts would include (make visible) new physics effects. The obtained ratio and cross section values for both leptonic and hadronic channels were given for two different centre of mass energies 7.08 TeV and 10 TeV in Table II and Table III, respectively. In the tables, the high ratio values correspond to the high suppression effect on the SM background. Evaluating Table II and Table III together, it was seen that there are almost no difference in the obtained ratio values for cut1 and cut2. This can be explained by the fact that a minimum of $p_t^\gamma > 20$ GeV cut-offs put into the transverse momentum of the photon between the two cuts do not suppress the SM contributions. On the other hand, examining at the ratio values along cut2-cut5, it was seen that the most striking increase was in cut5, which was put a $p_t^\gamma > 50$ GeV addition to cut1.

Considering all these findings, cut5 are discussed for the rest of our study. The dependence of the cross section of the $e^-p \rightarrow e^- \gamma^* p \rightarrow e^- W^+ b \gamma^* \rightarrow e^- j \bar{j} b \gamma^*$ and $e^-p \rightarrow e^- \gamma^* p \rightarrow e^- W^+ b \gamma^* \rightarrow e^- l \nu_l b \gamma^*$ processes on the new physics parameter λ_q for $\sqrt{s} = 7.08$ TeV and $\sqrt{s} = 10.0$ TeV is depicted in Figure 1 and Figure 2, respectively. As it can be seen from the figures, the cross-section values of hadronic processes are higher than ones of leptonic processes. Comparing the figures for the same anomalous coupling constant, it was observed that the cross section is also high when the centre-of-mass energy is high. In fact, this is an expected result, since the new physics terms contain high energy dependence. In addition, new physics contributions along with the increased anomalous coupling constant have shown an effect far above the SM cross section.

TABLE II. cuts.

$\sqrt{s} = 7.08 \text{ TeV}$				
	Cuts	$\sigma_{SM}(pb)$	$\sigma_{Tot}(pb)$	Ratio
Leptonic Channel	cut1	6.257×10^{-6}	6.55×10^{-5}	10.4
	cut2	3.389×10^{-6}	3.90×10^{-5}	11.5
	cut3	2.125×10^{-6}	2.748×10^{-5}	12.9
	cut4	1.396×10^{-6}	2.083×10^{-5}	14.9
	cut5	9.839×10^{-7}	1.79×10^{-5}	18.2
Hadronic Channel	cut1	1.826×10^{-5}	1.758×10^{-4}	9.6
	cut2	6.105×10^{-6}	6.262×10^{-5}	9.7
	cut3	1.37×10^{-6}	5.33×10^{-5}	10.2
	cut4	4.113×10^{-6}	4.745×10^{-5}	11.5
	cut5	2.826×10^{-6}	3.952×10^{-5}	14.0

TABLE III. cuts.

$\sqrt{s} = 10.0 \text{ TeV}$				
	Cuts	$\sigma_{SM}(pb)$	$\sigma_{Tot}(pb)$	Ratio
Leptonic Channel	cut1	1.354×10^{-5}	1.406×10^{-4}	10.4
	cut2	7.418×10^{-6}	8.748×10^{-5}	11.8
	cut3	4.854×10^{-6}	6.573×10^{-5}	13.5
	cut4	3.252×10^{-6}	5.287×10^{-5}	16.3
	cut5	2.382×10^{-6}	4.752×10^{-5}	19.9
Hadronic Channel	cut1	3.803×10^{-5}	3.07×10^{-4}	8.0
	cut2	2.134×10^{-5}	1.704×10^{-4}	8.0
	cut3	1.373×10^{-5}	1.168×10^{-4}	8.5
	cut4	9.615×10^{-6}	9.187×10^{-5}	9.5
	cut5	6.825×10^{-5}	7.841×10^{-5}	11.4

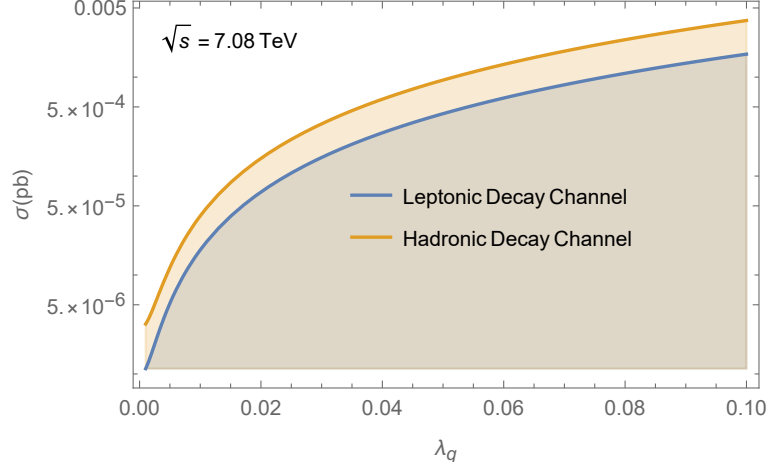


FIG. 1. The total cross sections of the processes $e^-p \rightarrow e^- \gamma^* p \rightarrow e^- W^+ b \gamma^* \rightarrow e^- j \bar{j} b \gamma^*$ and $e^-p \rightarrow e^- \gamma^* p \rightarrow e^- W^+ b \gamma^* \rightarrow e^- \nu_l b \gamma^*$ as a function of the anomalous λ_q coupling for center-of mass energy of $\sqrt{s} = 7.08 \text{ TeV}$ at the FCC-eh.

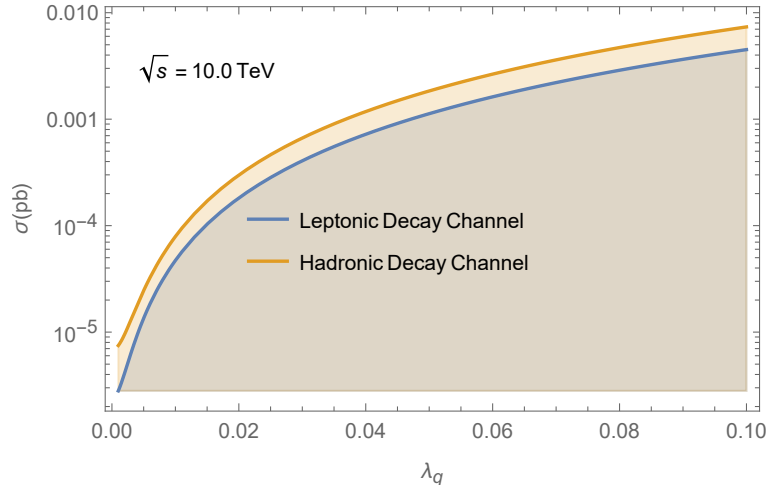


FIG. 2. The total cross sections of the processes $e^-p \rightarrow e^- \gamma^* p \rightarrow e^- W^+ b \gamma^* \rightarrow e^- j \bar{j} b \gamma^*$ and $e^-p \rightarrow e^- \gamma^* p \rightarrow e^- W^+ b \gamma^* \rightarrow e^- \nu_l b \gamma^*$ as a function of the anomalous λ_q coupling for center-of mass energy of $\sqrt{s} = 10.0 \text{ TeV}$ at the FCC-eh.

In this part of the study, we performed statistical analysis through the $e^-p \rightarrow e^- \gamma^* p \rightarrow e^- W^+ b \gamma^* \rightarrow e^- j \bar{j} b \gamma^*$ and $e^-p \rightarrow e^- \gamma^* p \rightarrow e^- W^+ b \gamma^* \rightarrow e^- \nu_l b \gamma^*$ processes with regard to examine sensitivity of anomalous λ_q couplings. We have used two different statistical analysis method depending on the number of SM events. If the number of SM events is ≤ 10 , the appropriate analysis method for this case is poisson analysis, while if the number of SM events > 10 , the chi-

square method is more suitable ones. In the Poisson analysis, the number of observed events is considered equal to the SM predictions, $N_{obs} = L_{int} \times b_{tag} \times \sigma_{SM} = N_{SM}$, b_{tag} symbolizes tagging efficiency and it is chosen 0.9. Here, we achieved Upper limits of the number of events N_{up} at 95% C.L. as follows,

$$\sum_{k=0}^{N_{obs}} P_{Poisson}(N_{up}, k) = 0.05 \quad (5)$$

On the other hand, the χ^2 function in the χ^2 criterion, without a systematic error is identify with following equation.

$$\chi^2 = \left(\frac{\sigma_{SM} - \sigma_{Tot}}{\sigma_{SM} \delta_{stat}} \right)^2 \quad (6)$$

where, σ_{SM} is the SM cross section, σ_{Tot} is the total cross section of process including additions from the Standard Model and New Physics. $\delta_{stat} = \frac{1}{\sqrt{N_{SM}}}$ shows the statistical error. In δ_{stat} , N_{SM} is identified by the formula of $N_{SM} = L_{int} \times b_{tag} \times \sigma_{SM}$, b_{tag} symbolizes tagging efficiency and it is chosen 0.9.

For sensitivity analysis, we have obtained constraints on the anomalous coupling parameter. In Table IV, it is represented results related $e^-p \rightarrow e^- \gamma^* p \rightarrow e^- W^+ b \gamma^* \rightarrow e^- j \bar{j} b \gamma^*$ and $e^-p \rightarrow e^- \gamma^* p \rightarrow e^- W^+ b \gamma^* \rightarrow e^- \nu_l b \gamma^*$ processes at centre-of-mass energy of 7.08 TeV for integrated luminosities 100,500,1000,1500,2000,3000 fb^{-1} . Whereas Table V is shown data about same processes and luminosities but for $\sqrt{s} = 10.0$ TeV.

Last part of the research is about the determination of the branching ratio limits on the anomalous $t \rightarrow q\gamma$ couplings. In these context, Figs 3 and 4 have been plotted $BR(t \rightarrow q\gamma)$ as a function of integrated luminosities via $e^-p \rightarrow e^- \gamma^* p \rightarrow e^- W^+ b \gamma^* \rightarrow e^- j \bar{j} b \gamma^*$ and $e^-p \rightarrow e^- \gamma^* p \rightarrow e^- W^+ b \gamma^* \rightarrow e^- \nu_l b \gamma^*$ processes. In these two graphs center-of-mass energy are accepted $\sqrt{s} = 7.08$ TeV and $\sqrt{s} = 10.0$ TeV, respectively.

According to the Figure 3 and Figure 4, it is inferred to computed constraints on $BR(t \rightarrow q\gamma)$ are better than the recent experimental data. For $\sqrt{s} = 7.08$ TeV (as it can be seen from the Fig3), even in $\mathcal{L} = 50 fb^{-1}$, the constraints obtained by the ATLAS collaboration were improved 2 and 3 times in both leptonic and hadronic channels, respectively. Also, for luminosity 1500 fb^{-1} value of the hadronic interaction process in the Figure 3, it was obtained $BR(t \rightarrow q\gamma) = 4.81 \times 10^{-6}$, which corresponds 50 times more improved than the final experimental results. While The BR value obtained in luminosity 3000 fb^{-1} for the hadronic channel are approximately 80 times better than the experimental result, this value

TABLE IV. 95% C.L. bounds on the anomalous $\lambda_{tq\gamma}$ coupling for center-of-mass energy $\sqrt{s} = 7.08$ TeV through the processes $e^-p \rightarrow e^- \gamma^* p \rightarrow e^- W^+ b \gamma^* \rightarrow e^- j \bar{j} b \gamma^*$ and $e^-p \rightarrow e^- \gamma^* p \rightarrow e^- W^+ b \gamma^* \rightarrow e^- \nu_l b \gamma^*$. It is taken under consideration integrated luminosities as 100,500,1000,1500,2000,3000 fb^{-1} .

$\sqrt{s} = 7.08$ TeV		
Hadronic Channel		Leptonic Channel
$\mathcal{L} (fb^{-1})$	$\lambda_{tq\gamma}$	$\lambda_{tq\gamma}$
100	0.0091164	0.0138035
500	0.0046133	0.00580993
1000	0.00400351	0.00504988
1500	0.00331624	0.00389067
2000	0.00289991	0.00388222
3000	0.0026536	0.00336868

TABLE V. 95% C.L. bounds on the anomalous $\lambda_{tq\gamma}$ coupling for center-of-mass energy $\sqrt{s} = 10.0$ TeV through the processes $e^-p \rightarrow e^- \gamma^* p \rightarrow e^- W^+ b \gamma^* \rightarrow e^- j \bar{j} b \gamma^*$ and $e^-p \rightarrow e^- \gamma^* p \rightarrow e^- W^+ b \gamma^* \rightarrow e^- \nu_l b \gamma^*$. It is taken under consideration integrated luminosities as 100,500,1000,1500,2000,3000 fb^{-1} .

$\sqrt{s} = 10.0$ TeV		
Hadronic Channel		Leptonic Channel
$\mathcal{L} (fb^{-1})$	$\lambda_{tq\gamma}$	$\lambda_{tq\gamma}$
100	0.00798568	0.00832519
500	0.00384720	0.0042881
1000	0.00301846	0.00323541
1500	0.00264058	0.00276383
2000	0.00238525	0.00248182
3000	0.00216549	0.00214141

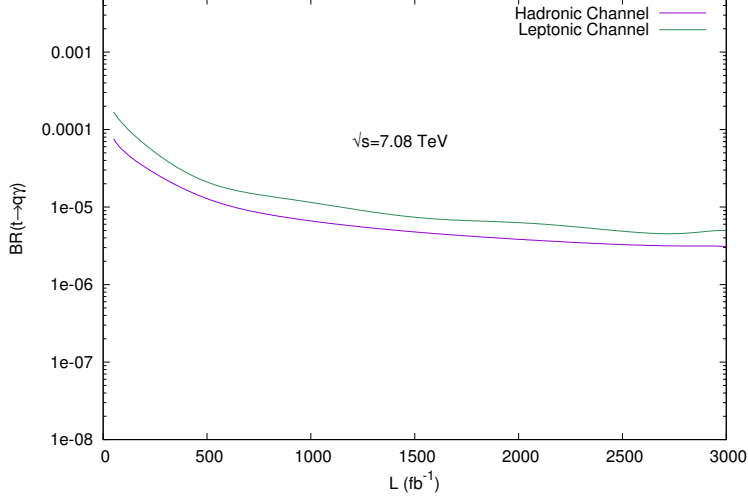


FIG. 3. For processes $e^+e^- \rightarrow e^+\gamma\gamma e^- \rightarrow e^+l\nu_l b\bar{q}e^-$ and $e^+e^- \rightarrow e^+\gamma^*\gamma^*e^- \rightarrow e^+l\nu_l b\bar{q}e^-$, 95% C.L. sensitivity limits on $BR(t \rightarrow q\gamma)$ for various integrated luminosities FCC-eh.

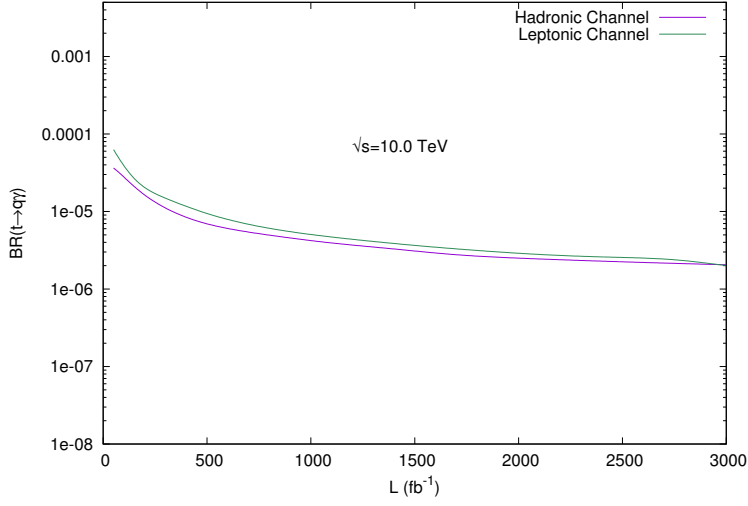


FIG. 4. Same as Fig3, but for center-of mass energy of $\sqrt{s} = 10.0$ TeV at the FCC-eh.

is also 1.60 times stronger than BR value for the leptonic channel. Since the centre of mass energy in Fig4 ($\sqrt{s} = 10.0 \text{ TeV}$) is larger than the ones in Fig3 ($\sqrt{s} = 7.08 \text{ TeV}$), better constraints were achieved on BR for $\sqrt{s} = 10.0 \text{ TeV}$. For the center-of mass energy of 10 TeV in the hadronic channel, the number of SM events at $\mathcal{L} \geq 1600 \text{ fb}^{-1}$ values is greater than 10. In this case, as mentioned before, two different analysis methods have been required. Hence, Poisson analysis was performed in the first part of the studies ($\mathcal{L} \leq 1600 \text{ fb}^{-1}$) while for the second part, ($\mathcal{L} \geq 1600 \text{ fb}^{-1}$), χ^2 analysis was conducted. According to the Fig 4, the hadronic

channel was more restrictive on $BR(t \rightarrow q\gamma)$ as same (Poisson) analysis up to luminosity $1600fb^{-1}$ was conducted for both hadronic and leptonic channel calculations. However, at luminosity greater than $1600fb^{-1}$ with increasing luminosity values, the difference between the BR limits closes and almost equalizes due to the use of different analysis methods for the two channel. To exemplify this situation, while for $\mathcal{L} = 1000fb^{-1}$, BR values are 4.59×10^{-6} for the leptonic channel and 3.99×10^{-6} for the hadronic channel $\mathcal{L} = 3000fb^{-1}$, BR values are 2.01×10^{-6} for the leptonic channel and 2.05×10^{-6} for the hadronic channel. In this context, the strictest limit obtained in the study is for the both hadronic and leptonic channel at an centre-of mass energy 10 TeV, at $3000fb^{-1}$ in FCC-eh conveyed in Fig4. This data is approximately 120 times the experimental limits reported by ATLAS Collaboration. In light of all these findings, in this paper, the experimental limits on the anomalous photon q branching of the top quark are restricted by two orders of magnitude.

IV. CONCLUSION

One of the most focused areas of scientists in research on new physics beyond the Standard Model is the examination of top quark interactions, the most massive particle of the SM. Also, it is well established that an interesting subject of top quark physics is FCNC transitions. Although this type of transition is prohibited in SM, it is allowed to be possible in some of the BSM models. However, there are no evidence about FCNC transitions under current experimental conditions. In the recent phenomenological studies, it hence has been focused on future colliders. In this context, our study are achieved the sensitivity limits for $tq\gamma$ coupling by considering $e^-p \rightarrow e^-\gamma^*p \rightarrow e^-W^+b\gamma^* \rightarrow e^-j\bar{j}b\gamma^*$ and $e^-p \rightarrow e^-\gamma^*p \rightarrow e^-W^+b\gamma^* \rightarrow e^-\nu_l b\gamma^*$ from the γq processes that occur as a result of electron-proton interactions in the FCC collider, which is planned to be built in the future. Furthermore, our results were compared with the recent experimental limits reported by ATLAS collaboration and found more restrictive than ATLAS collaboration's ones. Here, we observed that the obtained strictest limits were for $\sqrt{s} = 10.0$ TeV and $\mathcal{L} = 3000fb^{-1}$ in both the leptonic and hadronic processes. These results indicate improving of the experimental limits by 2 orders of magnitude. As a result, the future FCC-eh collider is promising for

detecting the presence of anomalous FCNC transitions.

- [1] G. Aad *et al.*, ATLAS Collaboration, Phys. Lett. B 716 (2012) 1.
- [2] S. Chatrchyan *et al.*, CMS Collaboration, Phys. Lett. B 716 (2012) 30.
- [3] M. M. Najafabadi, N. Tazik, Commun. Theor. Phys. 52 (2009) 662-664.
- [4] S. Khatibi, M. M. Najafabadi, Phys. Rev. D 89 (2014) 054011.
- [5] S. L. Glashow, J. Iliopoulos, and L. Maiani, Phys. Rev. D 2 (1970) 1285-1292 .
- [6] J. A. Aguilar-Saavedra and B. M. Nobre, Phys. Lett. B 553 (2003) 251.
- [7] J. L. Lopez, D. V. Nanopoulos and R. Rangarajan, Phys. Rev. D 5 (1997) 3100.
- [8] J. J. Cao *et al.*, Phys. Rev. D 75 (2007) 075021.
- [9] I. Baum, G. Eilam and S. Bar-Shalom, Phys. Rev. D 77 (2008) 113008.
- [10] D. Atwood, L. Reina and A. Soni, Phys. Rev. D 53 (1996) 1199.
- [11] G. P. K. Agashe and A. Soni, Phys. Rev.D 71 (2005) 016002.
- [12] S. Fajfer and J. F. Kamenik, JHEP 0712 (2007) 071.
- [13] J. J. Cao, et al., Phys. Rev. D 76 (2007) 014004.
- [14] H.-J. Zhang, Phys. Rev. D 77 (2008) 057501.
- [15] C.S. Li, R.J. Oakes, and T.C. Yuan, Phys. Rev. D 43 (1991) 3759.
- [16] Li X.-Q., et al., JHEP 1108 (2011) 075.
- [17] A. A. Ashimova and S. R. Slabospitsky, Phys. Lett. B 668 (2008) 282285.
- [18] O. Cakir *et al.*, Eur. Phys. J. C 70 (2010) 295-303.
- [19] O. Cakir, J. Phys. G, 29 (2003) 1181-1192.
- [20] Y. Zhang *et al.*, Phys.Rev. D 83 (2011) 094003.
- [21] R. Goldouzian, B. Clerbaux, Phys.Rev. D 95 (2017) 054014.
- [22] F. Larios *et al.*, Phys.Rev. D 72 (2005) 057504.
- [23] A. Cordero-Cid *et al.*, Phys.Rev. D 70 (2004) 074003.
- [24] J. Gao, C. S. Li, J. J. Zhang and H. X. Zhu, Phys. Rev. D 80 (2009) 114017.
- [25] P. M. Ferreira and R. Santos, Phys. Rev. D 80 (2009) 114006.
- [26] T. Han, J.L.Hewett, Phys. Rev. D 60 (1999) 074015.
- [27] T. Han, R.D.Peccei, X.Zhang, Nucl. Phys. B454 (1995) 527-540.
- [28] H.Sun, Nucl.Phys. B 886 (2014) 691-711.

- [29] M. Koksai, S. C. Inan, Adv. High Energy Phys. 2014 (2014).
- [30] K. Y. Oyulmaz, et al., Eur.Phys.J. C79 (2019) no.1 83.
- [31] I. Turk Cakir *et al.*, Adv. High Energy Phys. 2017 (2017) 1572053
- [32] H. Denizli *et al.*, Phys. Rev. D 96 (2017) no.1 015024.
- [33] O. Cakir *et al.*, arXiv:1809.01923.
- [34] Y. Guo, C. Yue, S. Yang, Eur. Phys. J. C76 (2016) no.11 596.
- [35] CLICdp Collaboration, CLICDP-PUB-2018-003, arXiv:1807.02441.
- [36] S. Khatibi, M. M. Najafabadi, Nucl.Phys. B 909 (2016) 607-618.
- [37] H. Khanpour *et al.*, Phys. Lett. B 775 (2017) 25-31.
- [38] S. C. Inan, Nucl. Phys. B 897 (2015) 289-301.
- [39] H. Khanpour, Nucl.Phys.B 958 (2020) 115141
- [40] T. Aaltonen *et al.*, CDF Collaboration, Phys. Rev. Lett. 102, (2009) 151801.
- [41] V. M. Abazov *et al.*, D0 Collaboration, Phys. Lett. B 701 (2011) 313.
- [42] T. Aaltonen *et al.*, CDF Collaboration, Phys. Rev. Lett. 101 (2009) 192002.
- [43] A. Heister *et al.*, ALEPH Collaboration, Phys. Lett. B 543 (2002) 173.
- [44] J. Abdallah *et al.*, DELPHI Collaboration, Phys. Lett. B 590 (2004) 21
- [45] G. Abbiendi *et al.*, OPAL Collaboration, Phys. Lett. B 521 (2001) 181.
- [46] P. Achard *et al.*, L3 Collaboration, Phys. Lett. B 549 (2002) 290.
- [47] The LEP Exotica WG, LEP Exotica WG 2001-01.
- [48] A. Aktas *et al.*, H1 Collaboration, Eur. Phys. J. C 33 (2004) 9.
- [49] ATLAS Collaboration, Phys. Lett. B 712 (2012) 351.
- [50] G. Aad *et al.*, ATLAS Collaboration, JHEP 1209 (2012) 139.
- [51] CMS Collaboration, JHEP 04 (2016) 035.
- [52] CMS Collaboration, JHEP 1806 (2018) 102.
- [53] ATLAS Collaboration, G. Aad et. al., Phys. Lett. B800 (2020) 135082, [1908.08461].
- [54] FCC Collaboration A. Abada *et al.*, Eur.Phys.J.C 79 (2019) 6, 474
- [55] FCC Collaboration A. Abada *et al.*, Eur.Phys.J.ST 228 (2019) 4, 755-1107
- [56] Y.C.Acar *et al.*, Nuclear Inst. and Methods in Physics Research, A 871 (2017)47-53.
- [57] O.Bruning, et al. (2017) CERN-ACC-2017-0019.
- [58] V. M. Budnev, I. F. Ginzburg, G. V. Meledin and V. G. Serbo, Phys. Rep. 15 (1975) 181.
- [59] G. Baur *et al.*, Phys. Rep. 364 (2002), 359 .

- [60] K. Piotrzkowski, Phys. Rev. D 63 (2001), 071502 .
- [61] J. Pumplin, D. R. Stump, J. Huston, H. L. Lai, P. M. Nadolsky and W. K. Tung, JHEP (2002) 0207 012.
- [62] A. Amorim, J. Santiago, N. Castro, and R. Santos, <http://feynrules.irmp.ucl.ac.be/wiki/GeneralFCNTop>, .
- [63] J. A. Aguilar-Saavedra, Nucl. Phys. B 812, 181 (2009) doi:10.1016/j.nuclphysb.2008.12.012 [arXiv:0811.3842 [hep-ph]].
- [64] J. A. Aguilar-Saavedra, Nucl. Phys. B 821, 215 (2009) [arXiv:0904.2387 [hep-ph]].
- [65] J. Alwall et al., JHEP 1407, 079 (2014) [arXiv:1405.0301 [hep-ph]].
- [66] A. Alloul, N. D. Christensen, C. Degrande, C. Duhr and B. Fuks, Comput. Phys. Commun. 185, 2250 (2014) [arXiv:1310.1921 [hep-ph]].